Kinetic Energy Release Distributions for Tropylium and Benzylium Ion Formation from the Toluene Cation†

D. Fati, A. J. Lorquet, R. Locht, J. C. Lorquet, and B. Leyh*

Department of Chemistry, University of Liège, Sart-Tilman, Building B6c, B-4000 Liège 1, Belgium

Received: May 6, 2004; In Final Form: June 10, 2004

Hydrogen loss from the toluene molecular ion generates benzylium (Bz^+) and tropylium (Tr^+) ions via two competitive and independent pathways. The corresponding kinetic energy release distributions (KERDs) have been determined under various conditions in the metastable time window for toluene and perdeuterated toluene and have been analyzed by the maximum entropy method (MEM). The isomeric fraction Tr^+/Bz^+ is found to be equal to 0.9 ± 0.3, in good agreement with the values obtained using photodissociation and charge exchange experiments. It is, however, in disagreement with the value 5 ± 2 deduced by Moon, Choe, and Kim (*J. Phys. Chem. A* **2000**, *104*, 458) from KERD measurements. The origin of the discrepancy is suggested to be the inadequacy of the orbiting transition state theory (OTST) for the calculation of KERDs in hydrogen loss reactions. For both channels, more translational energy is released in the reaction coordinate than would be expected on statistical grounds because of the presence of a barrier along the reaction path. For the Bz^+ channel, the barrier entirely results from centrifugal effects. Rotational energy is converted into translation as a result of angular momentum conservation. Deuteration is observed to reduce the importance of the rotational energy flow in the reaction coordinate. The Tr^+ channel is characterized by the presence of a reverse activation energy barrier of electronic origin. The energy in excess of the dissociation asymptote can be partitioned into two components: the reverse barrier plus a nonfixed energy contribution. About 40% of the reverse barrier is converted into relative translational motion of the fragments. Here again, a lower fraction of the nonfixed energy flows into translation for the deuterated isotopomer.

I. Introduction

According to the statistical theories of mass spectra,[1−8] a lifelong interest in Tomas Baer's outstanding career, the internal energy of an ionized molecule is completely randomized among all available degrees of freedom before dissociation takes place. In this statistical view, the internal energy is the only parameter that fully determines the unimolecular dissociation. The main argument is that the rate and the outcome of a unimolecular dissociation are usually observed to depend only on the total energy and not on how the molecule is activated.

Studies of the translational energy of separation of the two products of a decomposition have also often been said to support the statistical approach.[1−14] The most detailed information is provided by the function $P(\epsilon|E)$ that gives the probability of releasing a translational kinetic energy ϵ from a molecular ion having an excess internal energy E with respect to the dissociation asymptote. This function is termed the kinetic energy release distribution (KERD). It is a direct outcome of the detailed reaction dynamics of the system and can be expected to be related to the shape of the potential energy surface in the post-transition state region. Note that ϵ is defined in the molecular center of mass frame.

A variant of phase space theory,[15] termed orbiting transition state theory (OTST),[1,9,11,12] has been developed to predict KERDs when the potential energy increases steadily along the reaction path and does not show any reverse activation energy barrier (Type I reactions).[10,16] On the other hand, the presence of a reverse activation energy barrier (Type II reactions)[10,16] raises challenging problems. In general, reverse barriers lead to nonstatistical distributions because exit-channel effects play a leading role.[2,10] In that case, the energy in excess of the dissociation asymptote can be thought of as the sum of two components: one representing the reverse barrier plus a nonfixed energy contribution. Each of these components gives rise to a very different energy-sharing pattern.[17] Part of the reverse barrier potential is converted into relative translational energy and part of it is redistributed among all degrees of freedom. The nonfixed energy of the transition state does of course also contribute to the translational energy release, and this is usually expected to take place in a more statistical way.

Toluene constitutes an attractive system because its singly charged cation has been studied for years. A wealth of experimental data is already available on it, especially on its hydrogen loss reaction $C_7H_8^+ \rightarrow C_7H_7^+ + H$.[18−23] A thorough review of this process has been provided by Lifshitz.[23] Two dissociation energy pathways are in competition. They lead to the formation of either the benzylium (Bz^+) or the tropylium (Tr^+) ions. The Bz^+ ion is formed at its thermochemical threshold, since H abstraction from the toluene cation has no reverse activation energy.[23] However, the pathway leading to Tr^+ formation is much more complicated. A value of 0.43 eV has been calculated for the reverse activation energy for H abstraction from the cycloheptatriene radical cation.[22] Thus, although Tr^+ has been calculated to be 0.48 eV more stable than Bz^+, its appearance energy is not lower than that of Bz^+. The internal energy dependence of the dissociation rates $k(E)$ and of the isomeric ion ratio Tr^+/Bz^+ have also been measured.[18,20−23]

† Part of the special issue "Tomas Baer Festschrift".

* Corresponding author. E-mail: Bernard.Leyh@ulg.ac.be. Fax: ++32-4-3663413.

10.1021/jp048058d CCC: $27.50
Published on Web 07/27/2004

TABLE 1: Results of KERD Measurements at Three Values of the Fragment Translational Energy in the Laboratory Frame for the Toluene Ion and Its Perdeuterated Isotopomer[a]

	$C_7H_8^+ \rightarrow C_7H_7^+ + H$			$C_7D_8^+ \rightarrow C_7D_7^+ + D$		
V_{acc}	3 kV	5 kV	8 kV	3 kV	5 kV	8 kV
$\langle E \rangle$ (eV)	3.62	3.79	3.94	4.29	4.37	4.45
$\langle \epsilon \rangle$ (eV)	0.266	0.269	0.289	0.281	0.283	0.296
$\langle \epsilon^2 \rangle$ $(eV)^2$	0.021	0.020	0.027	0.022	0.019	0.024
f	0.55 ± 0.05	0.45 ± 0.05	0.55 ± 0.05	0.45 ± 0.05	0.5 ± 0.05	0.5 ± 0.05
λ_1 $(eV)^{-1/2}$	-8	-8	-8	-6	-6	-6
λ_1' $(eV)^{-1}$	-19	-15	-13	-21	-15	-16
λ_2' $(eV)^{-2}$	19	17	13	27	15	18
F_{Bz} (%)	51 ± 5	48 ± 5	45 ± 5	63 ± 5	62 ± 5	61 ± 5
F_{Tr} (%)	50 ± 5	69 ± 5	70 ± 5	64 ± 5	67 ± 5	68 ± 5

[a] $\langle E \rangle$, average internal energy sampled; $\langle \epsilon \rangle$ and $\langle \epsilon^2 \rangle$, first and second moments of the KERDs. Results of the fit to the maximum entropy eq 6.5: branching ratio f, Lagrange multipliers λ_1, λ_1', and λ_2', and ergodicity index F for the benzylium and tropylium channels.

Almost all investigations on the toluene system have focused mainly on the branching ratios and the rate constants. However, more recently, Moon et al.[13] have obtained the experimental KERD using mass analyzed ion kinetic energy spectroscopy and have then derived a branching ratio for the production of Bz^+ and Tr^+. The KERD of the Bz^+ pathway was theoretically calculated using OTST, and the KERD of the Tr^+ channel was then obtained by subtracting this calculated distribution from the experimental one. This analysis leads to an inconsistency with previous work since the Tr^+/Bz^+ branching ratio found by Moon et al. is much larger (5:1) than in other reports which give a ratio close to one at the internal energy investigated, i.e., about 3.3 eV with respect to the $C_7H_8^+$ ground state.[18,19,22,23]

It is therefore interesting to investigate further this issue with the help of the maximum entropy method (MEM), which has been developed to detect nonstatistical effects and which has been successfully used in detailed analysis of experimental KERDs.[24−34] This also gives us the opportunity to extend the application range of this methodology to competitive reactions involving a reverse activation barrier.[17]

II. Experimental and Data Handling

The KERDs for the $C_7H_8^+ \rightarrow C_7H_7^+ + H$ reaction are deduced from ion translational energy spectra recorded with a forward geometry two-sector mass spectrometer, in which the electrostatic analyzer is followed by the magnetic field. The accelerating voltage scan method[35] allows us to observe metastable dissociations taking place in the first field-free region (between the ion source exit slit and the electrostatic analyzer). In the experiments reported here, the electrostatic analyzer exit slit (β-slit) has been closed to 0.25 mm to reach an energy resolution $\Delta E/E$ of 10^{-3}. Accelerating voltage scan spectra have been recorded for fragment ion translational energies ranging between 3 and 8 keV (in the laboratory frame).

The shape of a metastable ion peak, in particular its width, reflects the translational kinetic energy released to the fragments, i.e., the KERD.[36−38] In addition, the experimental peak shapes obtained are further broadened owing to energy and angular spread of the parent ion beam and to the apparatus function of the electrostatic sector. Due to the smallness of the observed released translational energy, a deconvolution procedure using a Fourier transformation algorithm has been performed to obtain data free from these experimental broadening effects.

After the deconvolution step, the KERD has to be obtained as a function of the translational energy in the center-of-mass frame, ϵ. This distribution is denoted as $\tilde{P}(\epsilon)$ to emphasize that it corresponds in general to an average over the internal energy distribution of the dissociating ion. $\tilde{P}(\epsilon)$ is derived by differentiating the deconvoluted ion kinetic energy spectrum followed by a transformation of variables from the laboratory coordinates to the center-of-mass coordinates.[36−38] More elaborate data handling procedures are available.[39−41] In the present experiments, however, angular discrimination effects can be neglected because the translational energy carried by the fragment ion in the laboratory frame is small (loss of a hydrogen atom).

However, the noise filtering procedure associated with the Fourier transformation introduces some minor oscillations in the wings of the deconvoluted peak (Gibbs phenomena). To avoid these nonphysical oscillations that numerical differentiation would enhance, the deconvoluted peak has been fitted to a Holmes−Osborne function,[38] i.e., to the product of a Gaussian function with a third-order polynomial, prior to differentiation.

We have tested the reproducibility of the KERDs obtained by analyzing different sets of data recorded within a period of eight months. It should be noted that the experimental conditions and in particular the repeller potential were identical in these experiments. The first and second moments of the KERDs measured in our experiments for the hydrogenated ($C_7H_8^+$) and deuterated ($C_7D_8^+$) isotopomers are given in Table 1. They were found to be reproducible within 3% for the first moment and within 5% for the second moment.

The experimental conditions were as follows: trap current of the ionizing electrons, 30 μA; electron energy, 70 eV. To avoid collision-induced dissociations with the background gas, the mass spectrometer is differentially pumped and the pressure in the field-free regions was kept in the 10^{-8} mbar range. Toluene samples, C_7H_8 and C_7D_8, were provided by Aldrich (99.8% stated purity) and were used without further purification.

III. Internal Energy Distribution of the Metastable Parent Ions

The metastable fragmentations of ions in the field-free regions of a sector mass spectrometer provide good quality KERDs because the high translational energy of the precursor ion (keV range) induces an amplification of the energy released in the laboratory reference frame. However, in such experiments, there is no direct internal energy selection, but rather a time window within which the dissociation takes place. Based on the spectrometer geometry parameters and on the operating conditions, the ion entry and exit times, τ_1 and τ_2, can be easily calculated. As a consequence of this time selection, the ions are transmitted according to a transmission function $T(E)$ equal to

$$T(E) = B(E)\,[e^{-k(E)\tau_1} - e^{-k(E)\tau_2}] \qquad (3.1)$$

where $k(E)$ is the unimolecular dissociation rate constant and

TABLE 2: Ab initio Calculated Vibrational Frequencies and Rotational Constants (in cm^{-1}) of the Tropylium and Benzylium Ions and of Their Perdeuterated Isotopomers[a]

benzylium$^+$ ion (C_{2v}):
160; 330; 346; 404; 514; 587; 606; 620; 771; 793; 820; 954; 964; 965; 976; 989; 1013; 1065; 1098; 1164; 1174; 1311; 1343; 1378; 1431; 1457; 1526; 1548; 1611; 3055; 3092; 3096; 3098; 3114; 3116; 3147.
0.178; 0.093; 0.061.
d_7- benzylium$^+$ ion (C_{2v}):
144; 280; 296; 355; 437; 485; 490; 564; 642; 643; 719; 761; 781; 796; 823; 831; 844; 846; 850; 869; 926; 1036; 1050; 1238; 1299; 1390; 1457; 1476; 1569; 2231; 2284; 2286; 2291; 2307; 2312; 2348.
0.146; 0.079; 0.051.
tropylium$^+$ ion (D_{7h}):
216 (2); 423 (2); 543 (2); 638; 847; 857 (2); 865 (2); 978 (2); 1021 (2); 1038 (2);1212 (2); 1269 (2); 1394; 1470 (2); 1511 (2); 1580 (2); 3072 (2); 3080 (2); 3089 (2); 3094.
0.125 (2); 0.0625.
d_7-tropylium$^+$ ion (D_{7h}):
190 (2); 408 (2); 461 (2); 469; 662 (2); 803 (2); 807 (2); 810; 820 (2); 864 (2); 893 (2); 932 (2); 1076; 1258 (2); 1496 (2); 1507 (2); 2267 (2); 2274 (2); 2283 (2); 2288.
0.105 (2); 0.0525.

[a] Degeneracies characteristic of the D_{7h} point group are indicated in brackets.

$B(E)$ is a normalization constant. Thus, the transmission efficiency T depends on the rate constant which, in turn, depends on the internal energy E. Internal energies will henceforth be defined with respect to the vibrationless ground state of the toluene ion $C_7H_8^+$ (or $C_7D_8^+$).

For a metastable dissociation, the internal energy distribution of the precursor ions, $D(E)$, is given by the transmission coefficient, $T(E)$, multiplied by the ionization cross section, which can be approximated by the corresponding photoelectron spectrum, PES(E).

$$D(E) = T(E)\,\mathrm{PES}(E) \tag{3.2}$$

The rate constant $k(E)$ has been taken from the work of Dunbar.[21] It should be noted that the photoelectron spectrum of toluene is not flat in the internal energy region sampled in the toluene ion metastable dissociation experiments, so that it is necessary to take this factor into account.

IV. Quantum Chemical Calculations

Ab initio calculations have been carried out on the $C_7H_8^+$ ion by Lifshitz and co-workers.[22] Their value of 0.43 eV for the reverse activation energy leading to tropylium$^+$ + H has been adopted here. However, for the maximum entropy analysis to follow, data on the fragments are needed, too.

It was first checked that the reaction paths leading to Tr^+ and Bz^+ products are independent. In principle, the two isomeric fragments could interconvert into each other via a nonplanar intermediate. To ascertain this, B3LYP and QCISD ab initio calculations were carried out (via the GAUSSIAN 94 package[42]) with a 6-31G(d) basis set of atomic orbitals. Both calculations detected a transition state between the two isomers at 3 eV above the equilibrium geometry of the benzylium ion, i.e., higher than the energy domain sampled in our metastable experiments (i.e., 1.2−2.1 eV above the Bz^+ + H asymptote and 1.7−2.6 eV above the Tr^+ + H asymptote). Therefore, interconversion has not been taken into account in this work, and the two dissociation pathways have been considered not to interfere.

(1) Benzylium Ion (Symmetry C_{2V}). The $^1A_1$ ground state of the ion is found to be planar. The 36 vibrational frequencies (35 harmonic + 1 anharmonic, see below) and the three rotational constants of the benzylium ion have been calculated ab initio by the B3LYP/6-31G(d) method recommended by Scott and Radom.[43] The basis set included 119 basis functions. The results are given in Table 2. Comparison with experimental measurements carried out by Eiden et al.[44] is possible for thirteen of them. The agreement is very good (average accuracy of the order of 2%; up to 4% in the worst case). The normal mode observed at 627 cm^{-1} and calculated at 606 cm^{-1} is found to correspond to the torsion of the CH_2 group with respect to the phenyl ring. This mode has been treated as an anharmonic oscillator converging to a first-order saddle point, which is calculated to be located 2.08 eV above the equilibrium structure, and where the CH_2 group is perpendicular to the ring.

The density of states of the pair of fragments has been calculated by the Beyer−Swinehart direct-count method including rotations.[1,45] In addition, a planar triplet state has been calculated at 1.84 eV above the ground state. Its perpendicular conformation at 2.29 eV above the equilibrium geometry of the singlet ground state is a first-order saddle point. It plays no role in the dissociation mechanism.

The same procedure has been followed for the deuterated benzylium ion. The results are given in Table 2. The anharmonic vibrational frequency corresponding to the CH_2 torsion is calculated at 437 cm^{-1}.

(2) Tropylium Ion (Symmetry D_{7h}). The tropylium isomer has a regular seven-membered ring structure and many of its vibrations are doubly degenerate. The results of the ab initio calculations, at the same level as for the Bz^+ isomer, are given in Table 2. Here again the calculated frequencies compare well with the 10 experimental frequencies measured in both solid state and solution by Sourisseau and Hervieu,[46] as well as with those calculated at the Hartree−Fock level by Bandyopadhyay and Manogaran,[47] and with those calculated at various levels of theory by Lee and Wright.[48]

V. Maximum Entropy Method

A. Basic Equations. The maximum entropy method (MEM)[24−28] can be used to analyze the experimental KERD arising from the dissociation of the toluene ion. At a given internal energy E, the experimental KERD $P(\epsilon|E)$ should be compared with a reference distribution, termed the *prior distribution* and denoted as $P^0(\epsilon|E)$, which is defined as the KERD that would have been obtained in the case of a completely statistical dissociation. In this hypothetical situation, the only constraint is provided by the total energy conservation law, which implies that all isoenergetic product states are equally populated.

Because it is based on purely statistical arguments, the prior distribution can be derived from the densities of states of the reaction products. In a dissociation process, a part of the internal

energy E equal to ϵ flows into the relative translational motion of the pair of fragments, whereas the remainder is stored in their vibrational−rotational degrees of freedom. Because the density of translational states in a three-dimensional space is proportional to $\epsilon^{1/2}$, the prior distribution $P^0(\epsilon|E)$ is given by[24−28]

$$P^0(\epsilon|E) = C(E)\epsilon^{1/2}N(E - E^0 - \epsilon) \quad (5.1)$$

where E^0 is the internal energy corresponding to the dissociation asymptote, $C(E)$ is a normalization factor and $N(E - E^0 - \epsilon)$ represents the vibrational−rotational energy-level density of the pair of dissociating fragments.

However, the experimental KERD deviates from the purely statistical distribution $P^0(\epsilon|E)$ because of the influence of dynamical constraints. As a result, the energy sharing between the reaction coordinate and the bath of vibrational−rotational degrees of freedom is no longer statistical.

Consider now the following expression derived from the prior distribution

$$P(\epsilon|E) = P^0(\epsilon|E)\exp(-\lambda_0)\exp[-\sum_r \lambda_r A_r(\epsilon)] \quad (5.2)$$

where λ_0 and λ_r are Lagrange multipliers. The quantities A_r, which are usually expressed as powers of ϵ, are referred to as constraints or informative observables. It can be shown[24−28] that eq 5.2 represents a KERD where energy is randomized as extensively as allowed by the dynamical constraints that operate on the system. It corresponds therefore to the maximum entropy situation taking the dynamical constraints into account.

Equation 5.2 has also been demonstrated[49] to converge to an exact expression for the KERD. The power of the MEM is that it is found to fit adequately most experimental KERDs already with a limited number of constraints (up to two usually). This fit makes possible the identification of the constraints that prevent the reaction from being completely statistical.

To quantify the deviations with respect to the purely statistical situation, we consider first the entropy of the continuous distribution $P(\epsilon|E)$, which is is defined as

$$S(E) = -\int_0^{E-E^0} P(\epsilon|E)\left[\ln\frac{P(\epsilon|E)}{N(\epsilon|E)}\right] d\epsilon \quad (5.3)$$

where $N(\epsilon|E)$ is the density of states for a translational energy equal to ϵ and a fragment internal energy equal to $(E - E^0 - \epsilon)$ in the other degrees of freedom. Starting from this definition, an entropy deficiency is then introduced as the difference between the entropy of the prior distribution, S^0, and that of the actual distribution, S:

$$DS = S^0 - S = -\lambda_0 - \sum_r \lambda_r \langle A_r\rangle \quad (5.4)$$

where $\langle A_r\rangle$ is the average value of the constraint A_r:

$$\langle A_r\rangle = \int_0^{E-E^0} A_r(\epsilon)P(\epsilon|E)\, d\epsilon \quad (5.5)$$

A nonzero value for DS implies that the phase space sampled by the pair of fragments is reduced with respect to its maximum value. The entropy deficiency is a positive quantity related to the fraction F of phase space effectively sampled by[29,50]

$$F = \exp(-DS) \quad (5.6)$$

For a fully statistical dissociation (i.e., 100% phase space sampling), $DS = 0$ and $F = 1$.

The previous definitions have been given for a well-defined value E of the internal energy. However, as previously mentioned in section III, in the case of a metastable dissociation, the dissociating ions have a relatively broad distribution of internal energies D(E). Taking this into account, the measured KERD, denoted $\tilde{P}(\epsilon)$, is given by

$$\tilde{P}(\epsilon) = \int_{E^0+\epsilon}^{\infty} D(E)P(\epsilon|E)\, dE \quad (5.7)$$

Explicitly,

$$\tilde{P}(\epsilon) = \int_{E^0+\epsilon}^{\infty} D(E)P^0(\epsilon|E)\exp(-\lambda_0)\exp(-\sum_r \lambda_r A_r)\, dE \quad (5.8)$$

B. Fitting Procedure. It is common practice to use a least-squares-fitting algorithm in MEM studies for fitting the chosen functional form [here, eq 5.8 with a limited number of constraints] to the experimental data. The criterion for assessing the quality of the fit is the χ^2 index, which is defined as the sum of the squares of the differences between the experimental KERD and the chosen functional form with given values of the Lagrange parameters. The optimal values for these parameters are those that minimize χ^2.

Because the number of parameters to be fitted in the present study can be as large as four, the use of a black-box algorithm for finding the minimum of χ^2 is dangerous since it could lead to irrelevant values of the parameters deriving from local minima in the χ^2 multidimensional surface. It was therefore preferred to first calculate the complete χ^2 surface, whose dimensionality is equal to the number of parameters, and to plot appropriate cross-sections of it. Such cross-sections are displayed as a set of iso-χ^2 curves. In each case, the range of variation of the parameters was first chosen wide enough to make sure that the global minimum of the surface was identified. The procedure was then repeated with a finer mesh to improve the precision. An example is given in section VI.

VI. Results

In section IV, the reaction paths leading to the Tr^+ and Bz^+ products were found to be independent because the interconversion barrier is higher than the available internal energy. The two dissociation pathways can be considered separately. Thus, the experimental KERD reflects the weighted sum [f and $(1 - f)$] of two contributions, corresponding to the formation of the two isomeric structures.

$$\tilde{P}(\epsilon) = f\tilde{P}_{Bz}(\epsilon) + (1 - f)\tilde{P}_{Tr}(\epsilon) \quad (6.1)$$

where $\tilde{P}_{Bz}$ and $\tilde{P}_{Tr}$ represent the KERDs for the Bz^+ and Tr^+ channels, respectively.

A. Benzylium Channel. There is no problem for the benzylium channel, which displays no reverse activation barrier. After several tests that consisted of comparing the χ^2 values obtained for different constraints ($\epsilon^{1/2}$, ϵ, ϵ^2), the constraint on the benzylium dissociation pathway was identified to be $\epsilon^{1/2}$. The particular expression of eq 5.2 appropriate to the benzylium channel is thus

$$P_{Bz}(\epsilon|E) = P^0_{Bz}(\epsilon|E)\, e^{-\lambda_0}e^{-\lambda_1\epsilon^{1/2}} \quad (6.2)$$

where the prior distribution $P^0(\epsilon|E)$ is expressed as

$$P^0_{Bz}(\epsilon|E) = C_{Bz}(E)\epsilon^{1/2}N_{Bz}(E - E^0_{Bz} - \epsilon) \quad (6.3)$$

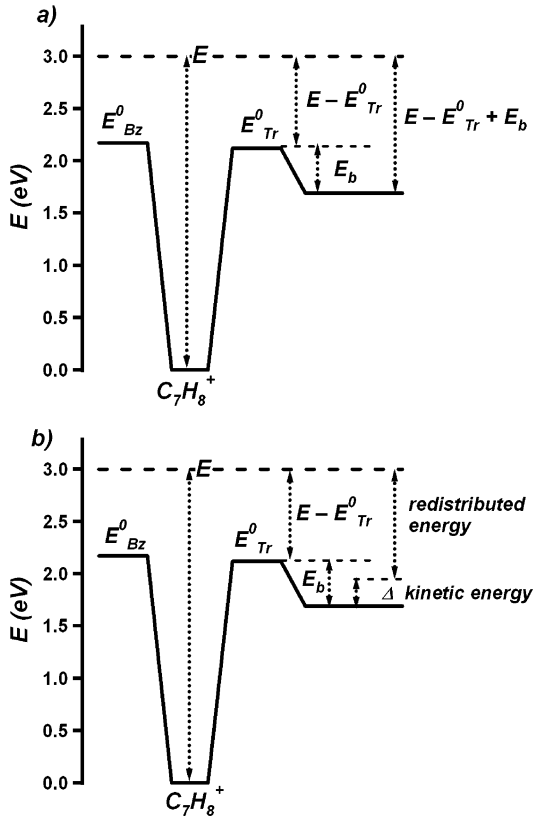

Figure 1. Schematic representation of two possible ways of partitioning the excess energy in the dissociation process leading to Tr^+. The zero of the energy scale is the vibrationless ground state of the toluene ion.

B. Tropylium Channel. The second channel leading to the Tr^+ fragment is quite another matter. It presents a reverse activation barrier (denoted E_b, see Figure 1) that introduces great difficulties into the analysis.

In principle, the total energy in excess of the dissociation asymptote, i.e., the quantity $E - E^0_{Tr} + E_b$, is available for redistribution among the relative translation and all internal degrees of freedom of the fragments (Figure 1a). Zamir and Levine[17] have proposed considering that the partitioning of both the reverse barrier E_b and the nonfixed contribution $E - E^0_{Tr}$ are governed by the same dynamical constraints. The constraints contribute differently to the value of the Lagrange parameter but their nature is the same. This approach has been adopted by Lorquet and Lorquet to analyze a translational energy distribution.[51]

The prior distribution for the Tr^+ channel is expressed as

$$P^0_{Tr}(\epsilon|E) = C_{Tr}(E)\epsilon^{1/2}N_{Tr}(E - E^0_{Tr} + E_b - \epsilon) \quad (6.4)$$

The description of repulsive releases by the maximum entropy method is known to require more than one constraint.[25] Therefore, several Lagrange multipliers are expected to be required to convert the prior distribution into an actual KERD via eq 5.2. Following the usual practice, the constraints have been expressed as powers (e.g., $\epsilon^{1/2}$, ϵ, ϵ^2) of the kinetic energy.

C. Complete Distribution. The full kinetic energy distribution $\tilde{P}(\epsilon)$ is a weighted sum of the Bz^+ and Tr^+ contributions. Because the energy domain defined by the internal energy distribution $D(E)$ is narrow, the Lagrange parameters and the isomeric fraction $(1 - f)/f$ can be considered to remain constant with energy. Different attempts showed that the overall KERD

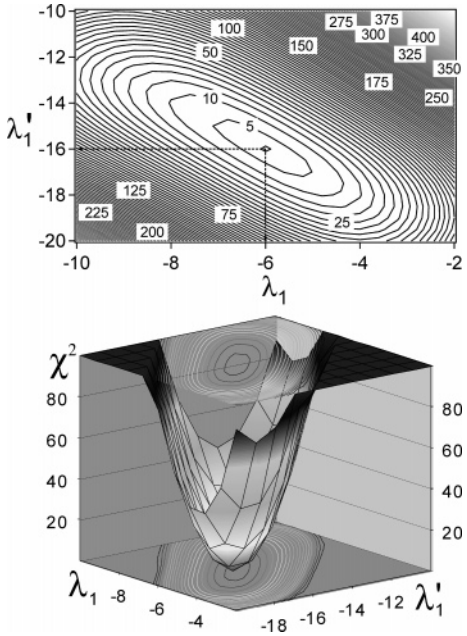

Figure 2. Example of least-squares fitting procedure. Top: Example of iso-χ^2 curves plotted as a function of the Lagrange multipliers λ_1 and λ_1' for fixed values of the branching ratio f and of the second multiplier λ_2'. Bottom: three-dimensional view of the χ^2 surface as a function of the same parameters.

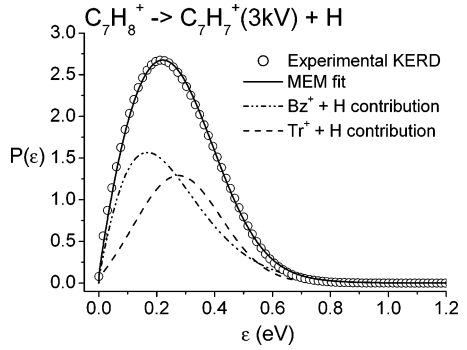

Figure 3. Experimental and fitted KERDs for the metastable dissociation of the toluene ion. Fragment ion translational energy in the laboratory frame equal to 3 keV. Open symbols: experimental results. Solid line: MEM fit. Dashed−dotted line: contribution of the Bz^+ channel. Dashed line: same for the Tr^+ channel.

is best described by the following equation, derived from eqs 5.8 and 6.1:

$$\tilde{P}(\epsilon) = f\int_{E^0_{Bz}+\epsilon}^{+\infty} D(E)P^0_{Bz}(\epsilon|E)\, e^{-\lambda_0}e^{-\lambda_1\epsilon^{1/2}}\, dE + (1 - f)\int_{E^0_{Tr}+\epsilon}^{+\infty} D(E)P^0_{Tr}(\epsilon|E)\, e^{-\lambda_0'}e^{-\lambda_1'\epsilon}e^{-\lambda_2'\epsilon^2}\, dE \quad (6.5)$$

Note that the values of the multipliers λ_0 and λ_0' are not adjustable unknowns in this equation: they are determined by normalizing separately each component.

Figure 2 illustrates the fitting procedure described in section VB. Iso-χ^2 curves are plotted as a function of the parameters λ_1 and λ_1' for given f and λ_2' values. This shows clearly how optimum values can be obtained for the Lagrange multipliers even if their number is as large as four.

Figures 3 and 4 show the experimental and the fitted distributions for the undeuterated and perdeuterated compounds. The obtained values of the parameters are given in Table 1. In particular, the branching parameter f is found to be of the order

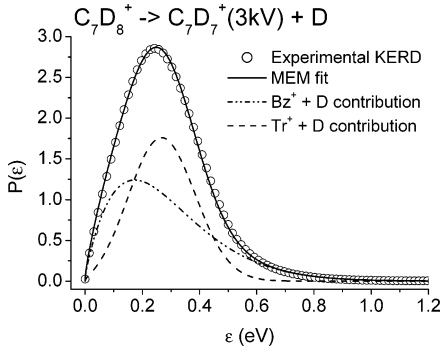

Figure 4. Experimental and fitted KERDs for the metastable dissociation of the perdeuterated toluene ion. Fragment ion translational energy in the laboratory frame equal to 3 keV. Open symbols: experimental results. Solid line: MEM fit. Dashed−dotted line: contribution of the Bz^+ channel. Dashed line: same for the Tr^+ channel.

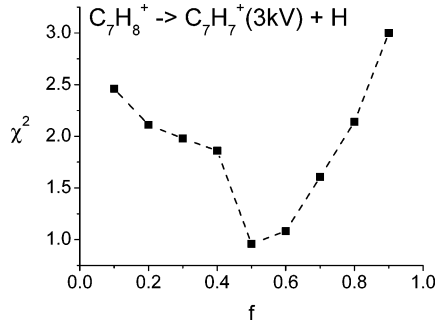

Figure 5. Determination of the branching ratio f by the least-squares method. At each f value, all other parameters are set at their least-squares optimized value.

of 0.5 (Figure 5), in agreement with the results obtained by Lifshitz,[22,23] Ausloos,[19] and Dunbar.[18]

To check the stability of the results, a second, more approximate model has been considered. In this model, as schematically illustrated in Figure 1b, it is assumed that a fixed part, Δ, of the reverse barrier, E_b, is not redistributed but is directly released as relative translational energy of the fragments. This generates a shift in the kinetic energy release curve by an amount Δ. $P_{Tr}(\epsilon|E)$ is then equal to zero for $\epsilon \leq \Delta$. As a result, a discontinuity in the derivative of the KERD is introduced at $\epsilon = \Delta$. The complementary part ($E_b - \Delta$) and the energy in excess of the barrier ($E - E^0_{Tr}$) are completely redistributed among all internal degrees of freedom.

Such a model has been previously adopted to analyze the reverse barrier contribution in the $C_6H_5Cl^+ \rightarrow C_6H_5^+ + Cl$ ($^2P_{1/2}$) dissociation.[32] The main drawback of this procedure is the discontinuity at $\epsilon = \Delta$, which, of course, is not observed in any experimental measurement.

The prior distribution for the Bz^+ channel is again given by eq 6.3. For the Tr^+ channel, it is piecewise defined:

$$P^0_{Tr}(\epsilon|E) = 0 \quad \text{for } \epsilon \leq \Delta$$
$$= C_{Tr}(E)\sqrt{\epsilon - \Delta}\,N_{Tr}(E - E^0_{Tr} + E_b - \epsilon) \quad \text{for } \epsilon \geq \Delta \tag{6.6}$$

The full kinetic energy distribution $\tilde{P}(\epsilon)$ is again a weighted sum of the Bz^+ and Tr^+ contributions. Assuming that a single constraint operates in each channel, one derives, from eqs 5.8, 6.1, 6.2, 6.3, and 6.6:

$$\tilde{P}(\epsilon) = f\int_{E^0_{Bz}+\epsilon}^{+\infty} D(E)P^0_{Bz}(\epsilon|E)\, e^{-\lambda_0} e^{-\lambda_1 \epsilon^{1/2}}\, dE + (1-f)\int_{E^0_{Tr}+\epsilon}^{+\infty} D(E)P^0_{Tr}(\epsilon|E)\, e^{-\lambda_0'} e^{-\lambda_1' \epsilon^{\alpha}}\, dE \tag{6.7}$$

This equation contains five unknown quantities: the isomeric branching ratio f, the shift Δ which appears in the prior distribution (eq 6.6), the Lagrange multipliers λ_1 and λ_1', and the unknown power α that adequately represents the constraint acting on the tropylium channel. The values of the multipliers λ_0 and λ_0' are determined by normalizing separately each component, as usual.

Several methods of fitting were tried. However, it turned out to be impossible to determine the value of these five unknowns by fitting eq 6.7 to the experimentally observed KERD. The origin of the difficulty is the discontinuity at $\epsilon = \Delta$ for the Tr^+ channel, which contributes significantly to the value of χ^2. Clearly, the higher the assumed contribution of the $Tr^+ + H$ pathway (that is, the lower the f value), the more significant the discontinuity zone. As a result, large Tr^+ contributions lead to artificially exaggerated χ^2 values. It is therefore not possible for this model to determine the Tr^+/Bz^+ branching ratio based on the χ^2 criterion, because large Tr^+ contributions are automatically penalized.

However, by setting the Tr^+/Bz^+ ratio to one (i.e., $f = 0.5$), in conformity with the data reported by Lifshitz,[23] we could estimate that the fraction of the reverse activation barrier that contributes to the kinetic energy release (i.e., the quantity Δ/E_b) is equal to 0.4 ± 0.1. This value compares well with other estimates given in the literature for systems of similar size. For example, for the dissociation of the protonated fluorobenzene, Lorquet and Lorquet[51] found that about $46 \pm 8\%$ of the barrier is released as kinetic energy. As will be seen in the discussion (section VII), this fraction is also compatible with the data obtained using eq 6.5. Also, the appropriate value of the exponent α is found to be equal to 1/2. Unexpectedly, the Lagrange multipliers λ_1 and λ_1' are found to be negative, which indicates that, for both channels, more translational energy is released in the reaction coordinate than the statistical expectation.

VII. Discussion

It has been shown in section VI how the experimentally observed KERD can be decomposed into two contributions resulting from the Bz^+ and Tr^+ dissociation pathways. The main features of each one are now discussed. However, this discussion and the confrontation of our results with earlier investigations[13,18,19,21−23] require that we first examine a more general question.

A. Validity of OTST. Considering the simple barrierless reaction leading to generation of Bz^+, Moon et al.[13] premised that "the statistical phase space theory provides a rather accurate prediction for KERDs in such a simple bond cleavage reaction". This statement has been questioned by Lifshitz.[5] We now wish to examine the reliability of OTST in the case of hydrogen loss reactions.

OTST is reliable only if the assumption of an isotropic ion-induced dipole potential is fulfilled, i.e., if the rotational barrier is located in a range where an effective potential can be defined in the form

$$V_{eff}(r) = -\alpha q^2/2r^4 + l^2/2\mu r^2 \tag{7.1}$$

where q is the charge carried by the ion, l is the orbital angular momentum, α is the polarizability of the released atom, and μ is the reduced mass of the pair of fragments.

For a hydrogen loss reaction, this condition can be fulfilled at very low energies only. This can be seen as follows. The distance r_c at which the effective potential $V_{eff}(r)$ has its maximum is related to l by the equation

$$r_c(l) = (2\mu\alpha q^2)^{1/2}/l \tag{7.2}$$

For hydrogen loss reactions, which are characterized by a small polarizability α and a small reduced mass μ, the maximum value of l is given by

$$l_{max} = (8\mu^2\alpha q^2\epsilon)^{1/4} \tag{7.3}$$

where ϵ is the kinetic energy that results from the conversion of the orbital barrier into translational energy. Substituting eq 7.3 into eq 7.2 leads to

$$r_c(\epsilon) = (\alpha q^2/2\epsilon)^{1/4} \tag{7.4}$$

In the toluene molecule, the distance between the center of the phenyl ring and one of the hydrogen atoms of the methyl group is about 3.45 Å. Therefore, OTST can meaningfully describe KERDs only up to a translational energy ϵ that fulfills the inequality

$$(\alpha q^2/2\epsilon)^{1/4} \gg 3.45 \text{ Å}$$

i.e., $\epsilon \ll 0.034$ eV! This result illustrates the inadequacy of OTST for the study of hydrogen loss reactions. In fact, the central field ion-induced dipole equation $V(r) = -\alpha q^2/2r^4$ starts to be credible when the distance between the center of mass of the benzylium ion and the hydrogen atom is larger than about 6 or 7 Å. This implies [eq 7.4] that the KERD calculated by OTST is valid up to 2 meV only! Hence, the procedure adopted by Moon et al.[13] to subtract a component calculated by OTST from an experimental KERD seems to us unreliable. A more extensive discussion of the validity of OTST for KERD calculations will be published elsewhere.

B. Benzylium Channel. For benzylium ion generation, both methods of analysis reported in the previous section essentially agree. The constraint bears on $\epsilon^{1/2}$, which has been already observed for barrierless reactions.[30−33] However, they also agree on the fact that the associated Lagrange multiplier λ_1 is negative, which means that more energy flows into the reaction coordinate than would be expected on statistical grounds. This situation is quite unusual: all barrierless reactions examined so far are characterized by a positive value of λ_1.[30−34] The observation that the kinetic energy release is smaller than the statistical share could be explained in terms of a "momentum gap law" (which can be viewed as a consequence of the Franck−Condon principle).[30,32,52,53] We suspect that the anomaly observed in the present case is again a hallmark of hydrogen loss reactions.

On the basis of reasons discussed below, we believe that rotational energy flow into the reaction coordinate is responsible for at least part of the observed behavior. The arguments are as follows. Marcus[54] has proposed to model the reacting molecule as a rigid prolate symmetric top with the two smaller rotational constants B and C equal ($A > B = C$). The rotational energy levels are then quantized according to the equation

$$E_{rot} = B\,J\,(J+1) + (A-B)\,K^2 \tag{7.5}$$

where the quantum number K measures the component of the angular momentum along the symmetry axis. Marcus then assumes the doubly degenerate rotation to be adiabatic, i.e., inactive in intramolecular energy transfer. His argument[45,54] is that these two degrees of freedom provide the major contribution to the strictly conserved angular momentum and therefore are approximately conserved. However, the argument is based on the principle of energy equipartition, which dates back to Eyring's postulate of thermodynamic equilibrium.

To dispense with the thermodynamic argument, it is preferable to invoke the influence of the symmetry properties of the system. There exists a conservation theorem which provides that the projection of the total angular momentum on the axis of symmetry is conserved when the system maintains cylindrical symmetry throughout the dissociation process.[55] We now proceed to show how, as a result of this theorem, rotational energy can flow into the reaction coordinate rather than to vibrational energy. The theorem is applicable to a unimolecular reaction only when the dissociation process is straightforward, i.e., when important structural rearrangements can be excluded. Note that the rotational constant B decreases all along the reaction coordinate, whereas A can be expected to remain approximately constant. Under this approximation, the degenerate external two-dimensional rotational energy is equal to $B\,J\,(J+1)$. As a result of the conservation of angular momentum, this quantity is unavailable for energy randomization with the vibrational degrees of freedom and is therefore termed inactive. The rotational barrier converts totally into rotational energy of the fragments only if $K = J$, whereas it converts into radial motion (i.e., into relative translational energy) when $K = 0$. Thus, the smaller K, the larger the fraction of the rotational barrier that is released as translational energy of the fragments.

Channeling an additional amount of translational energy in the reaction coordinate may account for a negative value of the Lagrange multiplier λ_1. As a rule, when both the polarizability α and the reduced mass μ of the pair of fragments are low, the centrifugal term dominates the influence of the electrostatic potential. Therefore, this effect is expected to show up only in hydrogen loss reactions. Even if K is not a strictly good quantum number for a particular symmetric top because of curvature and vibration−rotation coupling, some propensity can be thought to be present, i.e., a substantial part of the orbital barrier can be expected to be released as translational energy. Therefore, this effect should be conspicuous only for hydrogen loss reactions, because they are characterized by a large centrifugal barrier (of the order of the entire rotational energy). Loss of a massive particle such as iodine or bromine results in a very small barrier.

How good is the symmetric top model in the case of the reaction $C_7H_8^+ \rightarrow Bz^+ + H$? The rotational constants of toluene are equal to 0.185, 0.084, and 0.058 cm^{-1}.[56] The calculated constants of the benzylium ion do not differ greatly: $A = 0.178$ cm^{-1}, $B = 0.093$ cm^{-1}, $C = 0.061$ cm^{-1} (Table 1). Thus, neither the toluene nor the benzylium ions are good approximations to a symmetric top. However, what is needed are the rotational constants or moments of inertia of the complex $Bz^+ + H$ along the reaction path. The large rotational constant A is expected to vary smoothly betweeen 0.185 and 0.178 cm^{-1} and thus not to vary greatly. By contrast, it is easily seen that the moments of inertia corresponding to the other two rotations can be expressed as $h^2/2B + m_H\,D(D'+D)$ and $h^2/2C + m_H\,D(D'+D)$ where m_H is the mass of the hydrogen atom, and D and D' are the distances between the center of mass of the complex benzylium$^+$ + H and the center of mass of each moiety. Since D and D' increase steadily along the reaction coordinate, the symmetric top approximation can be expected to become reasonable in the range where the dynamics takes place. Thus, when the dynamics is dominated by the long-range part of the reaction path, the

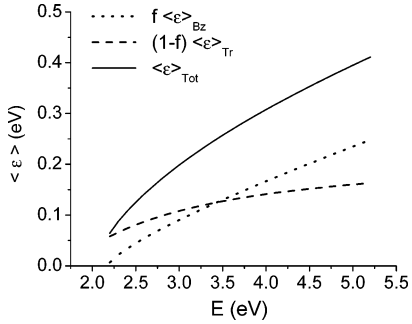

Figure 6. Solid line: average released translational energy $\langle\epsilon\rangle$ as a function of the internal energy E. Dotted and dashed lines: weighted contributions of the Bz^+ and Tr^+ channels, respectively.

symmetric top approximation should be adequate, which implies that angular momentum conservation should result in the release of a substantial amount of rotational energy into the radial motion.

If this interpretation is correct, then an isotope effect should be observed both on the value of the Lagrange multiplier λ_1 and on the ergodicity index F. The former goes from -8 $eV^{-1/2}$ (undeuterated) to -6 $eV^{-1/2}$ (deuterated) (Table 1), which means that the constraint becomes less efficient in the deuterated isotopomer. The ergodicity index F has been calculated for the benzylium channel via eqs 5.1−5.6. It increases from (48±8)% (undeuterated) to (62±6)% (deuterated). This shows that deuteration, which increases the reduced mass μ, increases the efficiency of phase space sampling by reducing the preferential flux of rotational energy into the relative translational motion.

Note the difference between the present argument and OTST. Both predict an efficient conversion of orbital energy into translation and point out that the energy flow will be particularly important for hydrogen loss reactions. However, the underlying mechanism is different. OTST breaks down when the ion-induced dipole central potential approximation becomes invalid. This is always the case for hydrogen loss reactions except at extremely low energies, as discussed in section VIIA. The mechanism presented here is based on the conservation of a cylindrical symmetry axis all along the reaction path.

C. Branching Ratio. The isomeric fraction Tr^+/Bz^+, expressed as $(1 - f)/f$, was found to be 0.9 ± 0.3 in the internal energy domain sampled, in good agreement with the values obtained using photodissociation[18] and charge exchange experiments[19] as well as with RRKM calculations.[22,23] It is, however, in disagreement with the value (5±2) given by Moon et al.[13] obtained by analyzing the KERD. We suggest that the origin of this discrepancy is the questionable assumption that the Bz^+ channel contribution can be calculated by OTST. The approach used in our work differs radically. Instead of calculating a theoretical KERD, we applied a MEM analysis to extract information from the experimental data. The Bz^+ channel contribution is found to be quite broad, far from statistical, and to have the same relative importance as the Tr^+ pathway contribution (Figures 3 and 4).

D. Partitioning the Average Kinetic Energy Release. In the framework of the maximum entropy method, the single internal energy KERD is given by

$$P(\epsilon|\mathrm{E}) = fP^0_{\mathrm{Bz}}(\epsilon|E)\, \mathrm{e}^{-\lambda_0}\mathrm{e}^{-\lambda_1\epsilon^{1/2}} + (1-f)P^0_{\mathrm{Tr}}(\epsilon|E)\, \mathrm{e}^{-\lambda'_0}\mathrm{e}^{-\lambda'_1\epsilon}\mathrm{e}^{-\lambda'_2\epsilon^2} \quad (7.6)$$

The average kinetic energy release, given in Figure 6 as a function of the internal energy of $C_7H_8^+$, is calculated as the first moment of this distribution

$$\langle\epsilon\rangle = \int_0^\infty \epsilon P(\epsilon|E)\, \mathrm{d}\epsilon \quad (7.7)$$

It is possible to partition the average kinetic energy release by expressing it as a weighted sum of the contribution of each isomer:

$$\langle\epsilon\rangle = f\langle\epsilon\rangle_{\mathrm{Bz}} + (1-f)\langle\epsilon\rangle_{\mathrm{Tr}} \quad (7.8)$$

where

$$\langle\epsilon\rangle_{\mathrm{Bz}} = \int_0^\infty \epsilon P^0_{\mathrm{Bz}}(\epsilon|E)\, \mathrm{e}^{-\lambda_0}\mathrm{e}^{-\lambda_1\epsilon^{1/2}}\, \mathrm{d}\epsilon \quad (7.9)$$

and

$$\langle\epsilon\rangle_{\mathrm{Tr}} = \int_0^\infty \epsilon P^0_{\mathrm{Tr}}(\epsilon|E)\, \mathrm{e}^{-\lambda'_0}\mathrm{e}^{-\lambda'_1\epsilon}\mathrm{e}^{-\lambda'_2\epsilon^2}\, \mathrm{d}\epsilon \quad (7.10)$$

The graphs corresponding to equations 7.8−7.10 are represented in Figure 6. The Bz^+ channel contribution is seen to dominate at high internal energy.

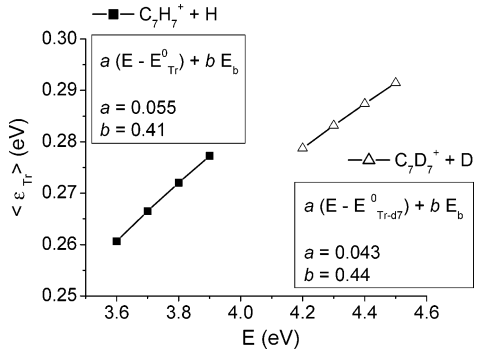

Figure 7. Average translational energy $\langle\epsilon\rangle$ released in the tropylium channel, as a function of the internal energy E, fitted to the sum rule expression. Filled squares: results for $C_7H_7^+ + H$. Open triangles: results for $C_7D_7^+ + D$.

E. Analysis of the KERD for the Tropylium Channel. The contribution of the Tr^+ channel to the experimental KERD is broader than its prior distribution and is shifted toward higher kinetic energies. This results from the presence of a reverse barrier in that channel, which shows itself in a release of kinetic energy larger than the statistical expectation.

Based on these data, an interesting analysis of the reverse barrier effect can be carried out. According to Zamir and Levine's "sum rule" approach,[17] the energy in excess with respect to the fragments can be split into two components: the energy of the barrier E_b and the nonfixed energy $(E - E^0_{\mathrm{Tr}})$. Then, the mean kinetic energy value for the Tr^+ dissociation pathway, $\langle\epsilon\rangle_{\mathrm{Tr}}$ can be expressed as

$$\langle\epsilon\rangle_{\mathrm{Tr}} = a(E - E^0_{\mathrm{Tr}}) + bE_{\mathrm{b}} \quad (7.11)$$

The coefficient a represents the part of internal energy in excess of the barrier that is converted into translational energy, while coefficient b determines the contribution of the barrier to the average translational energy. The inequality $b > a$ is expected because the energy of the barrier is preferentially released as translational energy. The internal energy in excess of the barrier $(E - E^0_{\mathrm{Tr}})$ contributes with a lower efficiency to the kinetic energy released.

Figure 7 gives the evolution of $\langle\epsilon\rangle_{\mathrm{Tr}}$ as a function of internal energy for the hydrogenated and deuterated isotopomers. Within the domain that corresponds to the internal energies sampled,

the "sum rule" expression (eq 7.11) has been fitted to the measured $\langle\epsilon\rangle_{Tr}$ values. For the nondeuterated species, one finds $a = 0.055 \pm 0.003$ and $b = 0.41 \pm 0.07$. For the deuterated isotopomer, $a = 0.043 \pm 0.003$ and $b = 0.44 \pm 0.07$.

The lower value of the coefficient *a* observed for the deuterated isotopomer indicates that for this species a lower fraction of the excess energy flows into translation. For the deuterated species the vibrational frequencies are lower than for the hydrogenated isotopomer. Therefore, at a given energy, the rovibrational density of states is higher for the deuterated species. In other words, in the deuterated isotopomer the translational energy is in competition with a higher density of rovibrational states and its share will be lower.

The value of *b* derived from the sum rule analysis indicates that 42±7% of the energy of the barrier is released as translational energy. This agrees with the result derived from the fit of the KERD to eq 6.7, which leads to the conclusion that about 0.4 ± 0.1 of the reverse barrier is released as relative translational energy. Similar orders of magnitude have previously been obtained for other reactions.[51,57−60] However, values of *b* of the order of up to 70% have been derived for reactions involving high reverse energy barriers.[61−63]

VIII. Concluding Remarks

The present study provides a contribution to the rich corpus of toluene and tropylium ion chemistry. By and large, the picture resulting in particular from the work of Lifshitz,[22,23] Dunbar,[18,21] and co-workers has been confirmed. However, it is equally interesting to try to generalize the obtained results. We had to deal with a competition between two unimolecular reactions. For one of them, we have tried to clarify the role played by a reverse activation barrier in the release of the translational energy. For the barrierless channel, the unreliability of OTST for hydrogen loss reactions has been emphasized. Some of our assertions have been substantiated by the observed isotope effect upon perdeuteration.

The reverse activation barrier along the pathway leading to Tr^+ requires the introduction of two constraints (ϵ and ϵ^2). In agreement with data on other molecular systems,[51,57−60] about 40% of the reverse activation barrier is released as relative translational energy of the fragments. The nonfixed energy is released to translation with a much smaller probability.

Possibly the most unexpected conclusion of the present work concerns the barrierless reaction leading to Bz^+. More translational energy is observed to be released in the reaction coordinate than predicted by statistical theory. Our interpretation suggests preferential flow of rotational energy in the reaction coordinate, resulting from the presence of a cylindrical symmetry axis during the dissociation process. However, for nonrigid systems such as a decaying molecule, conservation of the *K* quantum number has often been criticized, because its validity depends on the smallness of Coriolis interactions. This problem is best studied by the reaction path Hamiltonian method.[64−66]

At high internal energies, the dynamics takes place in a region where the ion-induced dipole potential is contaminated by anisotropic short-range valence contributions leading to a breakdown of the central field approximation. In the reaction path Hamiltonian method, the potential energy surface is modeled as a many-dimensional "harmonic valley" about the reaction path. The coordinates used in this model are *s*, the reaction coordinate (i.e., the arc length along the reaction path), plus $(3N - 7)$ normal coordinates that describe vibrations orthogonal to *s*. This procedure leads to a Hamiltonian that contains *s*-dependent coupling matrix elements. Some of them describe the Coriolis interaction, the remainder result from the curvature of the reaction path.

Miller et al.[64−66] could show that under reasonable conditions (moderate curvature, internal energy not too high) the vibrations can be expected to remain adiabatic, i.e., to show reluctance to transfer their energy to the reaction coordinate. For this reason, we feel that vibrational energy is much less likely to flow in the reaction coordinate than rotational energy. We intend to investigate that matter more fully in future work.

Acknowledgment. We are grateful to Ms. E. Gridelet for her assistance in some measurements and calculations. Financial support from the Belgian FNRS (Crédit aux chercheurs to B.L.) and by the Gouvernement de la Communauté Française de Belgique, via an "Action de Recherche Concertée" (ARC 99-04/245), is gratefully acknowledged.

References and Notes

(1) Baer, T.; Hase, W. L. *Unimolecular Reaction Dynamics. Theory and Experiments*; Oxford University Press: New York, 1996.
(2) Baer, T. *Adv. Chem. Phys.* **1986**, *64*, 111.
(3) Lifshitz, C. *J. Phys. Chem.* **1983**, *87*, 2304.
(4) Lifshitz, C. *Adv. Mass Spectrom.* **1989**, *11A*, 713.
(5) Lifshitz, C. *Adv. Mass Spectrom.* **1992**, *12*, 315.
(6) Lorquet, J. C. *Mass Spectrom. Rev.* **1994**, *13*, 233.
(7) Lorquet, J. C. *Int. J. Mass Spectrom.* **2000**, *200*, 43.
(8) Lorquet, J. C.; Leyh, B. Statistical theories in mass spectrometry. In *The encyclopedia of mass spectrometry*; Armentrout, P. B., Ed.; Elsevier: Amsterdam, 2003; Vol. 1; p 8.
(9) Leyh, B.; Lorquet, J. C. Kinetic energy release distributions in mass spectrometry. In *The encyclopedia of mass spectrometry*; Armentrout, P. B., Ed.; Elsevier: Amsterdam, 2003; Vol. 1; p 17.
(10) Laskin, J.; Lifshitz, C. *J. Mass Spectrom.* **2001**, *36*, 459.
(11) Chesnavich, W. J.; Bowers, M. T. Statistical Methods in Reaction Dynamics. In *Gas-Phase Ion Chemistry*; Bowers, M. T., Ed.; Academic Press: New York, 1979; Vol. 1; p 119.
(12) Chesnavich, W. J.; Bowers, M. T. *Prog. React. Kinet.* **1982**, *11*, 137.
(13) Moon, J. H.; Choe, J. C.; Kim, M. S. *J. Phys. Chem. A* **2000**, *104*, 458.
(14) Forst, W. *Unimolecular reactions. A concise introduction*; Cambridge University Press: Cambridge, 2003.
(15) Light, J. C. *Faraday Discuss. Chem. Soc.* **1967**, *44*, 14.
(16) Forst, W. *Theory of Unimolecular Reactions*; Academic Press: New York, 1973.
(17) Zamir, E.; Levine, R. D. *Chem. Phys.* **1980**, *52*, 253.
(18) Dunbar, R. C. *J. Am. Chem. Soc.* **1975**, *97*, 1382.
(19) Ausloos, P. *J. Am. Chem. Soc.* **1982**, *104*, 5259.
(20) Bombach, R.; Dannacher, J.; Stadelman, J. P. *J. Am. Chem. Soc.* **1983**, *105*, 4205.
(21) Huang, F. S.; Dunbar, R. C. *Int. J. Mass Spectrom. Ion Processes* **1991**, *109*, 151.
(22) Lifshitz, C.; Gotkis, Y.; Ioffe, A.; Laskin, J.; Shaik, S. *Int. J. Mass Spectrom.* **1993**, *125*, R7.
(23) Lifshitz, C. *Acc. Chem. Res.* **1994**, *27*, 138.
(24) Levine, R. D.; Bernstein, R. B. Thermodynamic Approach to Collision Processes. In *Dynamics of Molecular Collisions, Part B*; Miller, W. H., Ed.; Plenum: New York, 1976; p 323.
(25) Levine, R. D.; Kinsey, J. L. Information-Theoric Approach: Application to Molecular Collisions. In *Atom-Molecule Collision Theory. A Guide for the Experimentalist.*; Bernstein, R. B., Ed.; Plenum: New York, 1979; p 693.
(26) Levine, R. D. *Adv. Chem. Phys.* **1981**, *47*, 239.
(27) Levine, R. D. Statistical Dynamics. In *Theory of Chemical Reaction Dynamics*; Baer, M., Ed.; CRC Press: Boca Raton, FL, 1985.
(28) Levine, R. D.; Bernstein, R. B. *Molecular Reaction Dynamics and Chemical Reactivity*; Oxford University: New York, 1987.
(29) Levine, R. D. *Adv. Chem. Phys.* **1988**, *70*, 53.
(30) Urbain, P.; Leyh, B.; Remacle, F.; Lorquet, J. C. *Int. J. Mass Spectrom.* **1999**, *185/186/187*, 155.
(31) Urbain, P.; Remacle, F.; Leyh, B.; Lorquet, J. C. *J. Phys. Chem.* **1996**, *100*, 8003.
(32) Urbain, P.; Leyh, B.; Remacle, F.; Lorquet, A. J.; Flammang, R.; Lorquet, J. C. *J. Chem. Phys.* **1999**, *110*, 2911.
(33) Hoxha, A.; Locht, R.; Lorquet, A. J.; Lorquet, J. C.; Leyh, B. *J. Chem. Phys.* **1999**, *111*, 9259.
(34) Gridelet, E.; Locht, R.; Lorquet, A. J.; Lorquet, J. C.; Leyh, B. *Int. J. Mass Spectrom.* **2003**, *228*, 389.

(35) Barber, M.; Elliot, R. M. 12th Annual Conference on Mass Spectrometry and Allied Topics, 1964, Montreal.
(36) Beynon, J. H.; Fontaine, A. E.; Lester, G. R. *Int. J. Mass Spectrom. Ion Phys.* **1972**, *8*, 341.
(37) Cooks, R. G.; Beynon, J. H.; Caprioli, R. M.; Lester, G. R. *Metastable Ions*; Elsevier: Amsterdam, 1973.
(38) Holmes, J. L.; Osborne, A. D. *Int. J. Mass Spectrom. Ion Phys.* **1977**, *23*, 189.
(39) Rumpf, B. A.; Derrick, P. J. *Int. J. Mass Spectrom. Ion Proc.* **1988**, *82*, 239.
(40) Yeh, I. C.; Kim, M. S. *Rapid Comm. Mass Spectrom.* **1992**, *6*, 115.
(41) Szilagyi, Z.; Vekey, K. *Eur. Mass Spectrom.* **1995**, *1*, 507.
(42) Frisch, M. J.; Trucks, G. W.; Schlegel, H. B.; Gill, P. M. W.; Johnson, B. G.; Robb, M. A.; Cheeseman, J. R.; Keith, T.; Petersson, G. A.; Montgomery, J. A.; Raghavachari, K.; Al-Laham, M. A.; Zakrzewski, V. G.; Ortiz, J. V.; Foresman, J. B.; Peng, C. Y.; Ayala, P. Y.; Chen, W.; Wong, M. W.; Andres, J. L.; Replogle, E. S.; Gomperts, R.; Martin, R. L.; Fox, D. J.; Binkley, J. S.; Defrees, D. J.; Baker, J.; Stewart, J. P.; Head-Gordon, M.; Gonzalez, C.; Pople, J. A. *Gaussian 94*, rev. B.3; Gaussian, Inc.: Pittsburgh, PA, 1995.
(43) Scott, A. P.; Radom, L. *J. Phys. Chem.* **1996**, *100*, 16502.
(44) Eiden, G. C.; Lu, K. T.; Badenhoop, J.; Weinhold, F.; Weisshaar, J. C. *J. Chem. Phys.* **1996**, *104*, 8886.
(45) Gilbert, R. G.; Smith, S. C. *Theory of Unimolecular and Recombination Reactions*; Blackwell Scientific Publications: Oxford, UK, 1990.
(46) Sourisseau, C.; Hervieu, J. *Spectrochim. Acta* **1978**, *34A*, 881.
(47) Bandyopadhyay, I.; Manogaran, S. *J. Mol. Struct. (THEOCHEM)* **1998**, *432*, 33.
(48) Lee, E. P. F.; Wright, T. G. *J. Phys. Chem. A* **1998**, *102*, 4007.
(49) Alhassid, Y.; Levine, R. D. *J. Chem. Phys.* **1977**, *67*, 4321.
(50) Iachello, F.; Levine, R. D. *Europhys. Lett.* **1987**, *4*, 389.
(51) Lorquet, J. C.; Lorquet, A. J. *J. Phys. Chem. A* **2001**, *105*, 3719.
(52) Ewing, G. E. *J. Chem. Phys.* **1979**, *71*, 3143.
(53) Ewing, G. E. *J. Chem. Phys.* **1980**, *72*, 2096.
(54) Marcus, R. A. *J. Chem. Phys.* **1952**, *20*, 359.
(55) Goldstein, H. *Classical Mechanics*; Addison-Wesley: Reading, MA, 1950.
(56) Rudolph, H. D.; Dreizler, H.; Jaeschke, A.; Wendling, P. *Z. Naturforsch.* **1967**, *22a*, 940.
(57) Grandinetti, F.; Hrusak, J.; Schröder, D.; Karass, S.; Schwarz, H. *J. Am. Chem. Soc.* **1992**, *114*, 2806.
(58) Cacace, F.; Grandinetti, F.; Pepi, F. *Inorg. Chem.* **1995**, *34*, 1325.
(59) Aschi, M.; Grandinetti, F. *Eur. J. Mass Spectrom.* **2000**, *6*, 31.
(60) Choi, T. H.; Park, S. T.; Kim, M. S. *J. Chem. Phys.* **2001**, *114*, 6051.
(61) Aschi, M.; Cacace, F.; Grandinetti, F.; Pepi, F. *J. Phys. Chem.* **1994**, *98*, 2713.
(62) Aschi, M.; Grandinetti, F.; Pepi, F. *Int. J. Mass Spectrom. Ion Proc.* **1994**, *130*, 117.
(63) Lee, T. G.; Kim, M. S.; Park, S. C. *J. Chem. Phys.* **1996**, *104*, 5472.
(64) Miller, W. H.; Handy, N. C.; Adams, J. E. *J. Chem. Phys.* **1980**, *72*, 99.
(65) Miller, W. H. Reaction path Hamiltonian for polyatomic systems: further developments and applications. In *Potential energy surfaces and dynamics calculations*; Truhlar, D. G., Ed.; Plenum: New York, 1981; p 265.
(66) Miller, W. H. *J. Phys. Chem.* **1983**, *87*, 3811.